Effect of sonication time on the characteristics of nanophase hydroxyapatite crystals synthesised by the sol–gel technique

Songkot Utara[1], *Jutharatana Klinkaewnarong*[2]

[1]*Division of Chemistry, Faculty of Science, Udon Thani Rajabhat University, 64 Tahra Road, Muang, Udon Thani 4100, Thailand*
[2]*Program in Physics, Faculty of Science, Udon Thani Rajabhat University, 64 Tahra Road, Muang, Udon Thani 4100, Thailand*
E-mail: songkot_u@hotmail.com

Published in Micro & Nano Letters; Received on 6th June 2014; Accepted on 13th October 2014

An examination has been conducted of the effect of sonication time (25 kHz) at a constant temperature of 25°C on the structure of hydroxyapatite (HAp). Diammonium hydrogen phosphate and calcium nitrate tetrahydrate were used as starting materials. The gel formed by mixing the starting materials solution was subjected to sonication for 0, 5, 10, 20, 30 and 40 min. After sonication, HAp was dried at room temperature and calcined at 600°C for 2 h. The crystallisation, morphology and functional groups of the prepared nanoHAp were inspected by X-ray diffraction (XRD), transmission electron microscopy (TEM) and Fourier transform infrared (FTIR) spectroscopy. The XRD results revealed crystalline sizes in the range 50–58 nm and 3–5 of the crystalline fraction. The TEM results proved that the particle size of nano-HAp decreased with increasing sonication time. In addition, the FTIR spectroscopy confirmed that an increase of sonication time led to an increase in the concentration of carbonate groups

1. Introduction: Human bone is composed of 33–43% apatite materials, 32–44% organics and 15–25% water [1]. Hydroxyapatite ($Ca_{10}(PO_4)_6(OH)_2$, HAp) occurs in the bone mainly in platelet form, with a length of 40–60 nm, width of about 20 nm and thickness of 5 nm, arranged alongside collagen fibres [2]. Synthesised HAp is well known as a bioceramic material that can be used for hard tissue replacement because of its structure and composition being similar to that of mineralised human bone [3–4]. Many researchers have therefore attempted to synthesise HAp [1–4]. To improve the properties of synthesised HAp, this present research has improved the method of preparing HAp at nanoscale. It is well known that nanosized Hap, which has a grain size of less than 100 nm, has a high surface activity and ultrafine structure, similar to the mineral found in the bone tissues of humans [5]. Many studies have reported that a sono-chemical method is available for preparing nanosized HAp particles [1–8]. The advantages of this method are that fewer chemicals are used, with low cost, high phase purity, nanosized HAp and with narrow size distribution [5]. However, the ultrasonic apparatus used for preparing HAp has not been calibrated. In many papers, only the power input was given as a measure of the ultrasonication intensity, while ultrasonic reaction conditions (sample volume, distance between sample cell and transducer, diameter of ultrasonic probe) have not been reported [1–4]. Therefore the ultrasonic apparatus used for preparing HAp in this work was calibrated by means of KI oxidation dosimetry [9]. HAp nanoparticles were also synthesised using the sol–gel method with sono-chemical methods. In addition, the structure and morphology of the synthesised HAp powders were studied by X-ray diffraction (XRD), transmission electron microscopy (TEM) and Fourier transform infrared (FTIR) spectroscopy.

2. Experimental procedures

2.1. Calibration of ultrasonic reactor apparatus: An ultrasonic apparatus was set up as previously in our work [10]. The standard method used for the determination of sono-chemical efficiency (SE-value) is by means of KI oxidation dosimetry [9]. Deionised water was used for the preparation of 0.1 M KI. The reactor consists of an ultrasonic horn (diameter = 0.5 cm) which generates ultrasonic waves at 25 kHz and the power of the ultrasonic probe was 200 W. The Schlenk tube (100 cm^3, diameter 50 cm) was the reactor flask and its temperature was maintained at 25 ± 1°C by circulating thermostatically controlled water (10 dm^3) throughout the flask. The SE value of the reactor was 5.52×10^{-10} mol/J.

2.2. Hydroxyapatite preparation: Calcium nitrate tetrahydrate ($Ca(NO_3)_2{\cdot}4H_2O$) (4.15 g; 98%, Kanto Chemical) dissolved in ethanol (99.9%, Labscan Asian) was prepared (25 ml). Diammonium hydrogen phosphate ($(NH_4)_2HPO_4$) (5.90 g; 99%, BDH) was dissolved in deionised water (25 ml). Next, the two solutions were mixed in the Schlenk tube and placed in the ultrasonic reactor. The gap between the ultrasonic horn and the sample tube was

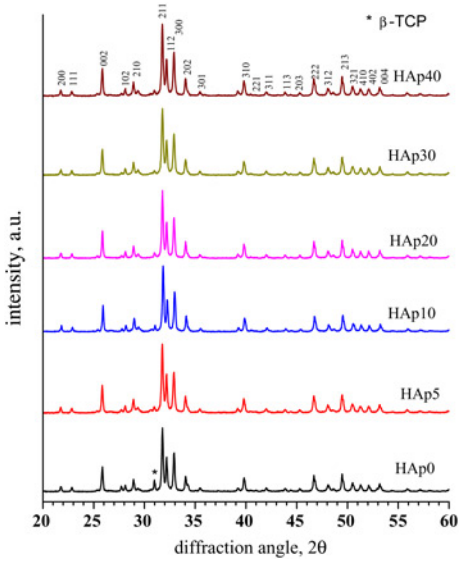

Figure 1 *XRD patterns of HAp powder as various sonication times compared with that of the standard data for pure HAp (ICCD No. 09–0432)*

Table 1 Parameters of HAp obtained from XRD line broadening calculated from XRD patterns of HAp sample

Nanocrystalline HAp	*d*-spacing, 211 nm	Crystallite size, nm	X_c
HAp0	0.28172	57.59 ± 6.25	4.60
HAp5	0.28170	50.13 ± 3.89	3.02
HAp10	0.28117	55.33 ± 3.52	4.02
HAp20	0.28162	57.53 ± 4.80	4.55
HAp30	0.28149	52.83 ± 6.75	3.63
HAp40	0.28165	55.27 ± 6.61	4.13

controlled at 0.5 cm. A white was precipitate formed and the mixture was continuously irradiated with ultrasonic waves for 0, 5, 10, 20, 30 and 40 min. Therefore the powder samples obtained at various sonication times were: HAp0, HAp5, HAp10, HAp20, HAp30 and HAp40, respectively. During the ultrasonic treatment, the temperature of the mixture was controlled at 25 ± 1°C. No pH adjustment was made throughout the whole process [11]. After the optimum time, the samples were allowed to age for 24 h at room temperature. The gel obtained was dried at 65°C for 24 h in a hot air oven (UF110, Memmert). In the next step, the powder for the dried gel was washed three times using deionised water to remove NH_4^+ and NO_3^-. Finally, the powder was calcined in a Muffle furnace (M12/14P, Chavachote) at 600°C at a heating rate of 3°C/

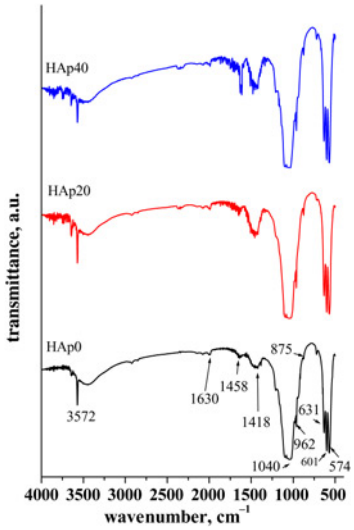

Figure 2 *Selected FTIR spectra of HAp powder at various sonication times*

min in air. The chemical reaction of HAp can be described by the following reaction

$$10Ca(NO_3)_2 \cdot 4H_2O + (NH_4)_2HPO_4 \rightarrow Ca_{10}(PO_4)_6(OH)_2 + 12NH_4NO_3 + 8HNO_3 + 38H_2O \quad (1)$$

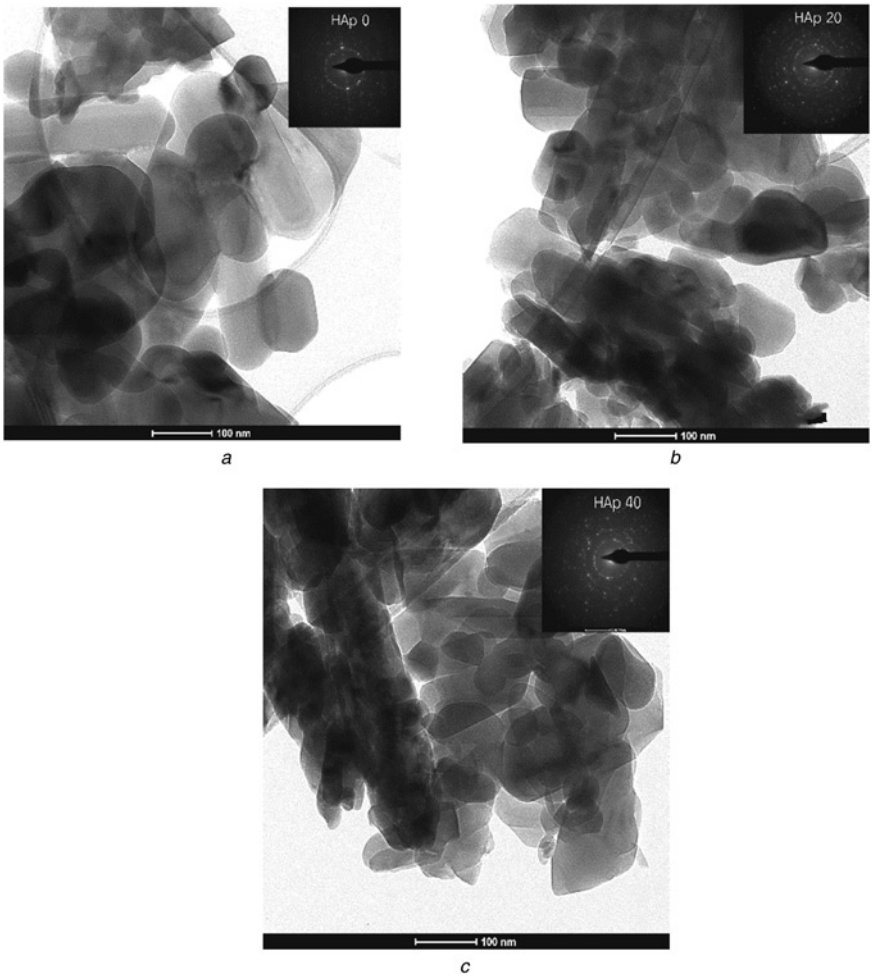

Figure 3 *TEM images with corresponding selected area electron diffraction (SAED) patterns of HAp powders calcined in air for 2 h at 600°C*
a HAp0
b HAp20
c HAp40

doi: 10.1049/mnl.2014.0316

2.3. HAp powder characterisation: The white powder obtained was ground into a fine powder and analysed using XRD, TEM and FTIR spectroscopy. XRD of all powder was carried out using D2 Phaser, Bruker AXS Analytical Instruments with Cu Kα radiation (λ = 0.15406 nm). The crystalline size (D) of the particles was calculated from the XRD line-broadening of the (002), (211), (300), (202), (310), (222) and (213) effects using the Debye-Scherrer's equation as follows [12, 13]

$$D = \frac{K\lambda}{\beta \cos\theta} \tag{2}$$

where K is a constant (0.89), λ is the wavelength (0.15406 nm), β is the full width at half maximum and θ is the diffraction angle. In addition, the fraction of the crystalline phase (X_c) of HAp was determined using the following equation [4]

$$X_c = \left(\frac{0.24}{\beta}\right)^3 \tag{3}$$

For the FTIR analysis, 1 mg of powder was mixed with 10 mg of KBr and palletised under vacuum. The powder sample was determined by FTIR spectroscopy (Shimazu, 809, Bara Scientific) in the range of 4000–500 cm^{-1} at a scan speed of 23 scan/min with 4 min^{-1} resolution. The morphology of the powder was observed by TEM (Tecnai G220, FEI, USA). The particle sizes of HAp were evaluated by analysis of the TEM images through ImageJ analysis (NIH) [14].

3. Results and discussion

3.1. XRD analysis: Broad-range XRD patterns of the calcined HAp powder in comparison with ICDD data are shown in Fig. 1. Phase peaks were observed around (002), (211), (300), (202), (310), (222) and (213) as the main phase of HAp matched well with the Powder Diffraction File (PDF Card No. 9–0432). No significant change can be seen in the main phase of HAp even while irradiating with different times. However, it was clearly observed that the β-tri-calcium phosphate (β-TCP) phase decreased with increasing sonication time. This result is consistent with that of Campos *et al.* [15], who found that the ultrasonic couple with the wet chemical method showed a lower intensity of β-TCP in comparison with that obtained by mechanical stirring. This finding indicates that ultrasonic radiation improves the purity of HAp [3]. The parameters of HAp obtained from XRD line broadening are shown in Table 1. The crystalline sizes observed from XRD line broadening were estimated to be 57.59 ± 6.25, 50.13 ± 3.89, 55.33 ± 3.52, 57.53 ± 4.80, 52.83 ± 6.75 and 55.27 ± 6.61 nm for HAp0, HAp5, HAp10, HAp20, HAp30 and HAp40, respectively. The d-spacing ranged from 0.28117 to 0.2172 nm and the fraction of the crystalline phase ranged from 3.02 to 4.60. From the work, no apparent relationship has been observed between sonication time and HAp crystallinity. However, decreased size and a lower fraction of crystallinity were observed in HAp5. Interestingly, in contrast to ultrasonic irradiation, a lower fraction of crystallinity of the ultrasonic couple was obtained using the sol–gel method.

Fig. 2 shows selected spectra of the calcined HAp0, HAp20 and HAp40. The bands at 3572 and 631 cm^{-1} are from the stretching, librational and translation modes of OH^- ion [16]. The bands at 962 and 1040 cm^{-1} arise from ν_1 PO_4^{3-} [16, 17] and ν_3 PO_4^{3-} [13, 16, 18]. The bands at 601 and 574 cm^{-1} result from ν_4 [16], the two peaks at 875 and 1418 cm^{-1} correspond to the CO_2^{3-} functional group [19]. Gopi *et al.* [3] suggested that the presence of the carbonate group is because of entrapment of atmospheric carbon dioxide during the stirring and calcination steps of the reaction. The broad band from about 3700 and 2500 cm^{-1} is associated with the ν_3 and ν_1 stretching modes of hydrogen-bonded H_2O

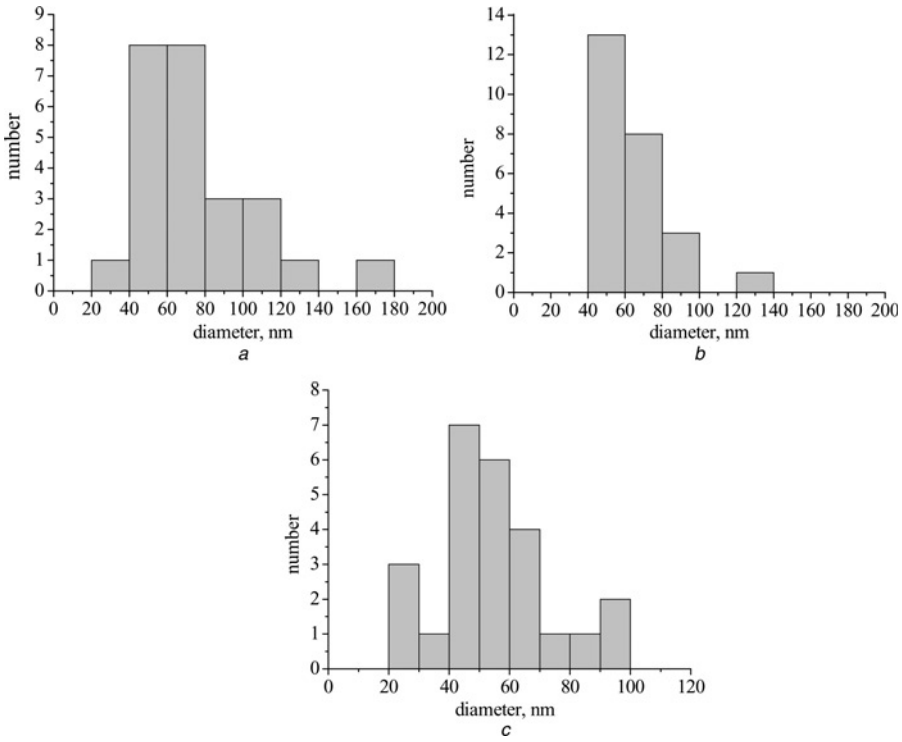

Figure 4 *Selected particle size distribution of powders calcined in air for 2 h at 600°C*
a HAp0
b HAp20
c HAp40

and the band at 1630 cm^{-1} is associated with the PO_4^3 v_2 bending mode of the H_2O molecules [16]. Interestingly, it was observed that the intensity of the CO_3^{2-} peak was more clearly observed with increasing sonication time.

The TEM images of the HAp samples are shown in Fig. 3. The HAp sample contained agglomerations of rod- and spherical-shaped particles. Moreover, the selected electron diffraction area has a stippled ring appearance, indicating random orientation of the crystalline components of HAp [11].

Using ImageJ calculation, the particle size distribution curves of HAp are shown in Figs. 4*a–c*. The particle size distribution curves were skewed in the case of HAp0 and HAp20. The narrow distribution range was obtained by an increase in sonication time. This result is consistent with that of Kim and Saito [8], who concluded that ultrasonic irradiation leads to the formation of very fine HAp particles with a relatively narrow size distribution. The average diameters (size distribution) of HAp0, HAp20 and HAp40 were found to be 75.60 ± 30.60, 65.30 ± 21.26 and 54.12 ± 19.27 nm, respectively. These results reveal that the average diameter decreased with increase in sonication time. These findings are consistent with those of Rouhani *et al.* [6], who found that the particles generated by sonication were generally smaller and more spherical than those obtained without sonication. In addition, Poinern *et al.* [7] also found that the longer ultrasonic contact time showed a decrease in the level of particle agglomeration, thus the average particle size decreased. The smallest HAp particles have a larger aggregate surface area, facilitating the adsorption of atmospheric CO_2. This explanation is congruent with the FTIR spectroscopy result (Fig. 2), which indicates that a higher intensity peak of CO_3^{2-} is observed at the longest sonication time.

4. Conclusion: Nano-HAp particles were prepared using the sol–gel method incorporating calibration of the ultrasonic reactor apparatus (5.52×10^{-10} mol/J). The optimum sonication time for producing a decreased crystalline size was 5 min. The crystalline size of HAp was found to be independent of sonication time. However, the 'average' particle size is dependent on the sonication time. A longer ultrasonic irradiation time for HAp resulted in a smaller HAp particle size. Normal particle size distribution in HAp was observed at longer ultrasonic contact times.

5. Acknowledgments: This work was supported by the Division of Chemistry and Program in Physics, Faculty of Science, Udon Thani Rajabhat University. The authors thank Asst. Prof. Dr. Aphiruk Chaisena for help with the FTIR spectroscopy measurement.

6 References

[1] Jevtic M., Mitric M., Skapin S., Jancar B., Ignjatovic N., Uskokovic D.: 'Crystal structure of hydroxyapatite nanorods synthesized by sonochemical homogeneous precipitation', *Cryst. Growth Des.*, 2008, **8**, (7), pp. 2217–2222

[2] Kuznetsov A.V., Fomin A.S., Veresov A.G., Putlyaev V.I., Fadeeva I. V., Barinov S.M.: 'Hydroxyapatite of platelet morphology synthesized by ultrasonic precipitation from solution', *Russ. J. Inorg. Chem.*, 2008, **53**, (1), pp. 1–5

[3] Gopi D., Govindaraju K.M., Victor C.A.P., Kavitha L., Rajendiran N.: 'Spectroscopic investigation of nanohydroxyapatite powder synthesized by conventional and ultrasonic couples sol-gel routes', *Spectrochim. Acta A, Mol. Biomol. Spectrosc.*, 2008, **70**, (5), pp. 1243–1245

[4] Gopi D., Indira J., Kavitha L., Sekar M., Mudali U.K.: 'Synthesis of hydroxyapatite nanoparticles by a novel ultrasonic assisted with mixed hollow sphere template method', *Spectrochim. Acta A, Mol. Biomol. Spectrosc.*, 2012, **93**, pp. 131–134

[5] Sadat-Shojai M., Khorasani M.T., Dinpanah-Khoshdargi E., Jamshidi A.: 'Synthesis methods for nanosized hydroxyapatite with diverse structure', *Acta Biomater.*, 2013, **9**, (8), pp. 7591–7621

[6] Rouhani P., Taghavinia N., Rouhani S.: 'Rapid growth of hydroxyapatite nanoparticles using ultrasonic irradiation', *Ultrason. Sonochem.*, 2009, **17**, (5), pp. 853–856

[7] Poinern G.E., Brundavanam R.K., Mondinos N., Jiang Z.T.: 'Synthesis and characterisation of nanohydroxyapatite using an ultrasound assisted method', *Ultrason. Sonochem.*, 2009, **4**, (3), pp. 469–474

[8] Kim W., Saito F.: 'Sonochemical synthesis of hydroxyapatite from H_3PO_4 solution with $Ca(OH)_2$', *Ultrason. Sonochem.*, 2001, **8**, (2), pp. 85–88

[9] Koda S., Kimura T., Kondo T., Mitome H.: 'A standard method to calibrate sonochemical efficiency of an individual reaction system', *Ultrason. Sonochem.*, 2003, **10**, (3), pp. 149–156

[10] Utara S., Moonart U.: 'Effect of frequency and sonication time on ultrasonic degradation of natural rubber latex', *Adv. Mat. Res.*, 2013, **747**, pp. 721–724

[11] Klinkaewnaron J., Swatsitang E., Maensiri S.: 'Nanocrystalline hydroxyapatite powders by a chitosan–polymer complex solution route: synthesis and characterization', *Solid State Sci.*, 2009, **11**, (5), pp. 1023–1027

[12] Cao L.Y., Zhang C.B., Huang J.F.: 'Synthesis of hydroxyapatite nanoparticles in ultrasonic precipitation', *Ceram. Int.*, 2005, **31**, (8), pp. 1041–1044

[13] Sanosh K.P., Chu M.C., Balkrishnan A., Kim T.N., Cho S.J.: 'Preparation and characterization of nano-hydroxyapatite powder using sol-gel technique', *Bull. Mater. Sci.*, 2009, **32**, (5), pp. 465–470

[14] Pathi S.P., Lin D.D.W., Dorvee J.R., Estroff L.A., Fischbach C.: 'Hydroxyapatite nanoparticle-containing scaffolds for the study of breast cancer bone metastasis', *Biomaterials*, 2011, **32**, (22), pp. 5112–5122

[15] Campos M.D., Muller F.A., Bressiani A.H.A., Bressiani J.C., Greil P.: 'Sonochemical synthesis of calcium phosphate powders', *J. Mater. Sci., Mater. Med.*, 2007, **18**, (5), pp. 669–675

[16] Markovic M., Fowler B.O., Tung M.S.: 'Preparation and comprehensive characterization of a calcium hydroxyapatite reference material', *J. Res. Natl. Inst. Stand. Technol.*, 2004, **109**, (6), pp. 553–568

[17] Castro F., Kuhn S., Jensen K., *ET AL.*: 'Continuous-flow precipitation of hydroxyapatite in ultrasonic system', *Chem. Eng. J.*, 2013, **215–216**, pp. 979–987

[18] Eslami H., Hashjin M.S., Tahriri M., Bakhshi F.: 'Synthesis and characterization of nanocrystalline hydroxyapatite obtained by the wet chemical technique', *Mater. Sci-Poland.*, 2010, **28**, (1), pp. 5–13

[19] Cimdina L.B., Borodajenko N.: 'Research of calcium phosphate using Fourier transform infrared spectroscopy', in Theophile T. (Ed.): 'Infrared Spectroscopy-Material Science, Engineering and Technology', ISBN: 978–953–51–0537-4, In Tech, DOI:10.5772/36942, http://www.intechopen.com/books/infrared-spectroscopy-materials-science-engineering-and-technology/research-of-calcium-phosphates-using-fourier-transformation-infrared-spectroscopy, accessed 20 May 2012

doi: 10.1049/mnl.2014.0316